Kanjirakkad. 2017. *Int. J. Turbines and Sustainable Energy*, 1(1), 1-7

doi: 10.4273/ijtse.1.1.01

International Journal of Turbines & Sustainable Energy
Available online at www.maftree.org/eja

Experimental Study of Endwall Flow in a Low-Speed Linear Compressor Cascade: Effect of Fillet Radius

Vasudevan Kanjirakkad

Thermo-Fluid Mechanics Research Centre, University of Sussex, United Kingdom

ABSTRACT:

This paper describes the study of endwall flow modification due to the presence of fillet radius in axial compressor blades. A fillet is commonly used at the intersection between the blade and the endwall in axial turbomachinery blade-rows to improve the mechanical integrity by reducing the local stresses. Since the endwall region is affected by secondary flow, separation and vortices the presence of the fillet can potentially modify the flow mechanism that results, especially, in the endwall blade corner region. In this paper an experimental study into the effects of the fillet, namely, the modification of the secondary flows and the generation of the losses under a low Reynolds number condition is discussed. It has been shown that, for the range of cases tested, employment of a uniform blade fillet reduces the overturning secondary flow. The measurements reported in the paper show no detrimental effects due to the presence of the fillet but on the contrary finds that the endwall and mass averaged losses are marginally lower compared to when no fillets are employed.

KEYWORDS:

Compressor; Cascade; Fillet; Loss

CITATION:

V. Kanjirakkad. 2017. Experimental Study of Endwall Flow in a Low-Speed Linear Compressor Cascade: Effect of Fillet Radius, *Int. J. Turbines & Sustainable Energy*, 1(1), 1-7. doi:10.4273/ijtse.1.1.01.

NOMENCLATURE AND ABBREVIATIONS:

C	Blade chord (m)
P	Pressure, (Pa)
Re	Reynolds number (chord based)
Y_p	Total pressure loss coefficient
h	Blade height (m)
s	Blade pitch, (m)
α	Flow angle (degrees)
β	Blade angle (degrees)
δ	Boundary layer thickness
χ	Stagger angle
ψ	Static pressure rise coefficient
CD	Controlled diffusion blading
DCA	Double circular arc blading
PS	Blade pressure side
SS	Blade suction side
$*_1$, $*_2$	Cascade inlet and exit static conditions
$*_{01}$, $*_{02}$	Cascade inlet and exit total conditions

1. Introduction

Aero-designers of gas turbine engines are constantly tasked with the unenviable task of efficiency improvement with every new design or platform development. Whilst our improved understanding of the underlying flow mechanisms is the key to better aerodynamic designs, improvements are possible using a variety of techniques some of which stem from developments outside the field of aerodynamics; metallurgy and material science, manufacturing and structural modelling, high-speed computing etc. The advent of high-speed computing and the exponential increase in number-crunching capabilities year-on-year, allowing for complex calculations to be performed ever faster, means that we can now look into the effects of geometrical features that were traditionally neglected or considered to be of secondary importance during the design process. Whole passage optimisation to account for features such as inter-platform gaps, strip seals, blade leading edge imperfections, manufacturing and assembly tolerances, endwall non uniformities etc. are now regularly attempted to look for 'lost' percentages of efficiency.

The presence of a compressor fillet at the joint between the blade aerofoil surface and the endwall (hub/casing) is one such feature the aerodynamic effect of which is not fully understood. Not surprisingly, there is not a great deal of published literature on this matter either. A reasonable number of studies are reported that shed light on the effect of fillet radius on turbine blades (Zess and Thole [1], Germain et al [2], Turgut and Camci [3], Mank et al [4], etc.) most of which are in the context of endwall profiling for performance enhancement. While the authors who studied a combination of endwall profiling and leading edge fillets claimed reduced losses at blade exit in some cases, the fillet radius on its own was found to increase loss proportionately with its size. Most studies reported a weakening of the secondary flow at the inlet due to the presence of a large fillet and a removal of the corner vortex if a fillet was present further downstream. The general message from such studies was that fillet effects need to be explicitly studied to get a closer understanding of the aerodynamics involved.

In the case of compressor blade fillets, however, there are not many publications addressing the aerodynamic effects. The effect of fillet radius of varying sizes (0%, ~6% and ~12% fillet radii expressed in terms of blade span) was investigated on a linear compressor cascade, fitted first with controlled diffusion (CD) blades and then with double circular arc (DCA) blades, by Curlett [5]. The author reported that for the CD blades the losses steadily went up with the size of the fillet and therefore one should aim to keep the fillet radius as minimum as possible for this type of blading. The DCA blades, however, were found to suffer no loss in performance with the addition of fillets. At low incidences the changes in loss with fillet radius was found to be negligible. At high incidences the fillet was found to produce 'measurably lower' losses. One interesting result from the above study was that the CD blades were found to produce higher losses near the blade midspan region when fillets were present but lower losses near the endwall compared to the no-fillet case.

However the reverse trend was found to be true for the DCA blades. The author attributed the higher endwall loss of no-fillet CD blade to a weaker corner vortex. The low loss near the mid-span of filleted DCA blades was attributed to a thinner blade boundary layer caused by increased velocities (i.e. higher axial velocity ratio caused by the fillet). It is, however, perplexing that a weaker corner vortex could produce higher losses. Also it is unclear why there is lower mid-span loss at higher velocities. The increased advantage of using a fillet at higher incidences was also shown by Kügeler et al [6] who numerically investigated a multistage compressor with blade fillets. In their test case, at higher incidences the flow at the blade leading edge stagnates on the pressure side causing larger corner separation on the suction side corner and an early stall. The study showed that this effect is minimised when a fillet is present as it allows smooth entry of the flow at the inlet. They also observed a reduced horse-shoe vortex formation.

Goodhand and Miller [7] who studied the impact of various real-geometry features in compressors also looked at the effect of fillets on the extent of blade corner separation. The leading edge fillet effect was examined by changing the fillet radius and also using a 'cut-away' fillet to simulate manufacturing imperfections. The effect of these changes at the leading edge on the hub separation was found to be negligible. The above authors also looked at the effect of employing a range of fillet radii around the blade (0%. 1.6%, 3.2%, 4.8% and 10% of chord). This study found that when a fillet is present the spanwise size of the hub separation increased with the fillet size. Removing the fillet altogether increased the extent of separation in all cases except for the 10% fillet for which the loss was closer to the no-fillet case. Additionally, the hub loss for the 4.8% fillet was found to be lower than that for the no-fillet case at design and off-design conditions.

Meyer et al [8] reported the aerodynamics associated with fillet radii in a high speed compressor cascade.Along with the no-fillet case they tested three different fillet sizes (2.5%, 7.5% and 10% of chord). For both the inlet Mach numbers tested (0.5 and 0.66) the total pressure loss was found to increase with fillet size. The losses were higher for the higher Mach number case. The secondary flow features on the suction side was found to migrate radially outward due to the displacement effect of the fillet. This resulted in higher losses at the mid-span and lower losses at the endwall region. For fillet radii that are below the boundary layer thickness it was found that there was an increase in static pressure rise. The authors argued that this was a result of an increased cross flow, when the fillets were present that reduced the axial velocity near the endwall resulting in a pressure rise. In the present study aerodynamic measurements are conducted in a low speed linear cascade facility which employs an identical blade shape as in the study by Meyer et al [8]. The objective is to understand the modification of the endwall flow due to the presence of the blade fillet, but at a much lower Reynolds number compared to the study by Meyer et al.

Throughout the tests reported in this paper an inlet velocity of 20 m/s was used and this corresponded to a Reynolds number of approximately 110,000. This is relatively low even for the rear stages of present day aeroengine compressors under cruise conditions. However, these conditions could still exist during off design operation such as start-up or hot-restarts in the event of an emergency engine shut off in mid-air. In the future, there is potential demand for the design of smaller and efficient engines to fit low-noise podded engine aircrafts and land based gas turbines for distributed power generation. Compressors with very low radii are therefore required in the rear stages and low Reynolds number operation would become inevitable. Loss generation and static pressure rise are looked at for three different fillet radii namely; 5%, 7.5% and 10% of the blade chord in addition to the datum case with no fillet. The rational for testing these fillet heights was that this allowed for a sensitivity analysis with respect to the inlet boundary layer thickness (δ) which was measured to be 7.5% (6 mm) of the chord. All fillets tested have a uniform radius around the blade.

2. Experimental methodology

The experiments were conducted in a low-speed linear cascade consisting of three blades and four passages. The blade shapes are based on the NACA65 family of vanes used in the University of Darmstadt axial compressor test rig. The 2-D profile used here is extracted from 10% span of the above vane. Albeit the use of only three blades, the cascade used here is a scaled version of the geometry used in the study by Meyer et al [8] that was mentioned earlier. Fig. 1 shows a schematic of the cascade arrangement. The airflow is sourced from a screw type rotary compressor. Prior to reaching the test section the air goes through a drier and a settling chamber. Since the ducting upstream of the cascade has an unavoidable elbow bend a series of gauzes are installed downstream of the elbow to make the flow uniform as it arrives at the inlet to the cascade. A combination of four pitot-tubes and static pressure taps installed at 5 blade chords upstream of the cascade inlet measures the inlet flow conditions. A calibrated 3-hole probe is traversed at a distance of 70% blade chord

downstream of the aerofoil trailing edge to survey the blade exit flow field. A traverse gear with three axes of freedom is used for this purpose. The linear cascade geometric parameters and test flow conditions are summarised in Table 1.

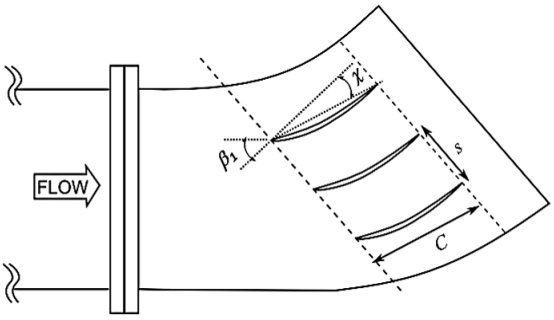

Fig. 1: Linear compressor cascade arrangement schematic

Table 1: Cascade parameters and test flow conditions

Parameter	Value
Blade chord, *C*	80mm
Blade pitch, *s*	44mm
Blade aspect ratio, (*h/C*)	1
Inlet blade angle, β_1	42°
Stagger angle, χ	15.2°
Inlet flow velocity, V_1	20m/s
Reynolds number, *Re*	106667
Inlet boundary layer thickness, δ	6mm

An acceptable level of periodicity was achieved despite the fact that only three blades were employed in the cascade as seen from the total pressure coefficient distribution at the cascade exit in Fig. 2. The central blade is used for detailed measurements, the results of which are, presented in the rest of the paper. The fillets are only built into the middle blade. A type of modelling clay was used to form the fillet evenly around the blade base. A scraping tool with an appropriate corner radius was used to the shape the clay around the blade when the clay remained workable. No fillet is present on the other blades on either side of the central blade.

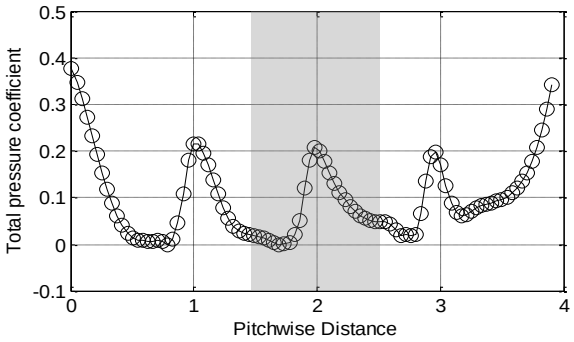

Fig. 2: Total pressure coefficient at mid-height across the cascade exit (the shaded region marks the test blade)

3. Results and discussion

The results from 3-hole probe area traverses conducted downstream of the aerofoil trailing edge are presented in this section. Firstly, the flow periodicity of the cascade was tested by carrying out a one-dimensional line traverse at mid-height across the whole pitch of the cascade and the result of this is already presented in Fig. 2. The detailed area traverses are only conducted downstream of the middle blade (shaded region in Fig. 2). The pitchwise extent of the traverse is one blade-pitch and the spanwise extent is from the near endwall where the fillet is applied to the blade mid-height location. The traverse grid consists of 20 spanwise positions and 25 pitchwise positions both having non-uniform grid spacing. The total pressure loss between the inlet and the exit of the cascade is presented in the form of a loss coefficient defined as:

$$Y_p = (P_{01} - P_{02})/(P_{01} - P_1) \quad (1)$$

Here P_{01} and P_1 refer to the inlet total pressure and static pressure, respectively, measured using the pitot-tubes and static tappings installed in the inlet duct as described earlier. P_{02} is the measured total pressure at the cascade exit using the 3-hole probe. The static pressure rise at the cascade exit was similarly defined using a coefficient:

$$\psi = (P_2 - P_1)/(P_{01} - P_1) \quad (2)$$

Here P_2 refers to the exit static pressure as measured by the 3-hole probe.

The total pressure loss coefficient (Y_p) contours at the exit of the cascade for the three fillet radii cases tested and for the datum test case with no fillet are shown in Fig. 3. For clarity only contour lines between the values of 0.1 and 0.225 are shown with an interval of 0.025. The main features present in all the contour plots are the blade wake, the endwall boundary layer and the loss-core and vortex (visible in Fig. 4) associated with the secondary flow. Although the contour plots look similar, close inspection would show quantitative differences. The location of the secondary loss-core at around 26% span for the no-fillet case is found to marginally drop (towards the endwall) to around 24% span when the smallest of the fillet with 4 mm radius is applied. As the fillet radius is increased to 6 mm and then to 8 mm, the loss-core is seen to gradually migrate radially outward by approximately 2% of span each time. This observation is in agreement with that of Meyer et al [8] who attributed the radial migration to the 'displacement effect' introduced by the fillet.

But the 'inward' movement of the loss-core when the 4 mm fillet was introduced, compared to the no-fillet case, in the present study, suggests that the mere presence of the fillet alone is not responsible for this radial displacement but it is more likely a result of the modification of the endwall flow by the fillet. Evidently the 'folded' region where the loss-core interacts with the endwall fluid is more compressed for the 4 mm fillet compared to the no-fillet case. This becomes less compressed as the fillet size is increased. Consequently the width of the widest part of the loss region just above the endwall boundary layer (at approximately 2-3% span) increases slightly for the 4 mm fillet case and then 'thins' significantly as the fillet size increases. The wake region near the mid-span is approximately 3% wider for the 4 mm fillet case compared to the no-fillet case. But as the fillet size is increased to 6 mm and 8 mm the wake near the mid-span becomes thinner by 3% and 6% respectively. This observation of wake thinning is similar to that made by Curlett [5] for the DCA blades.

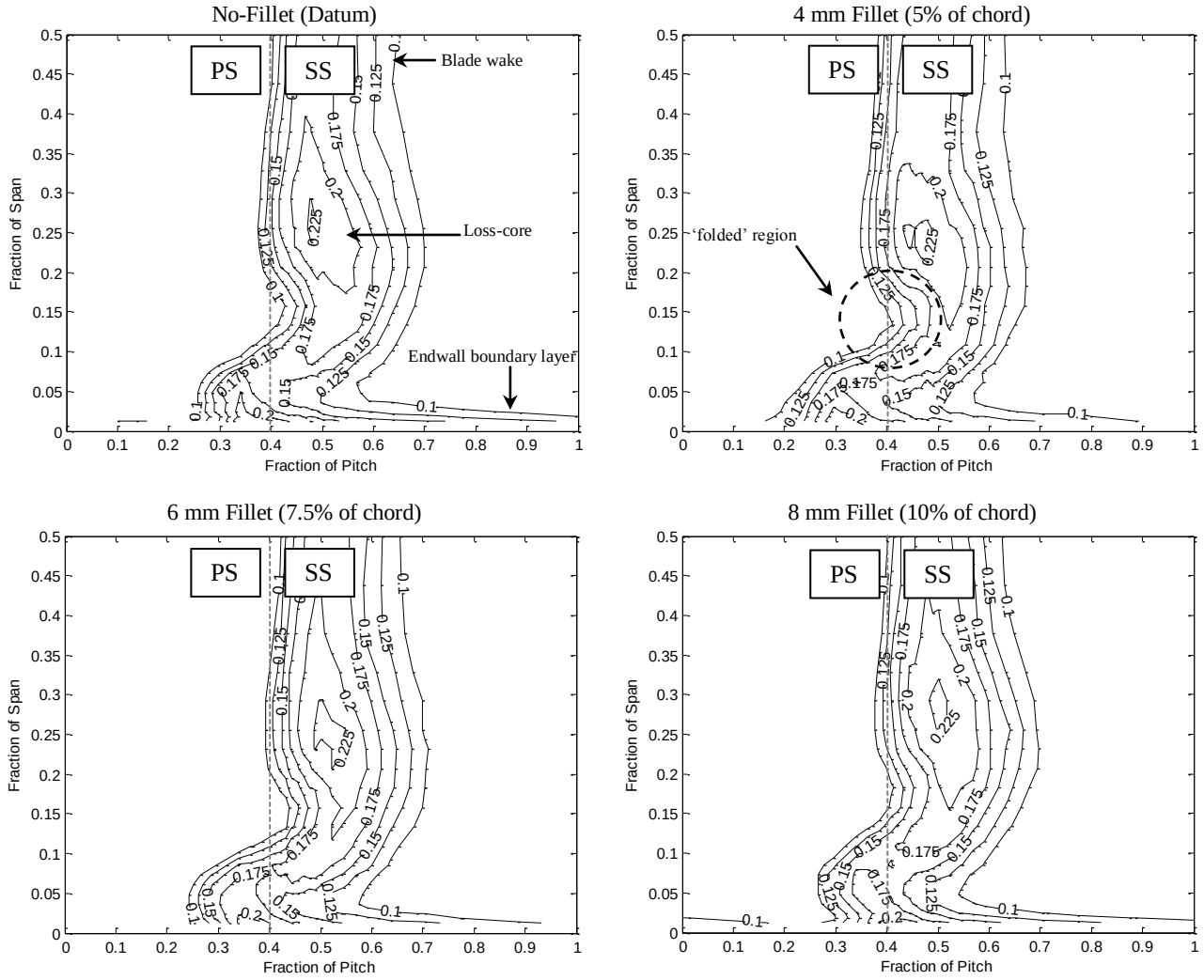

Fig. 3: Contours of total pressure loss coefficient for different tip gaps at cascade exit (70% blade chord from trailing edge)

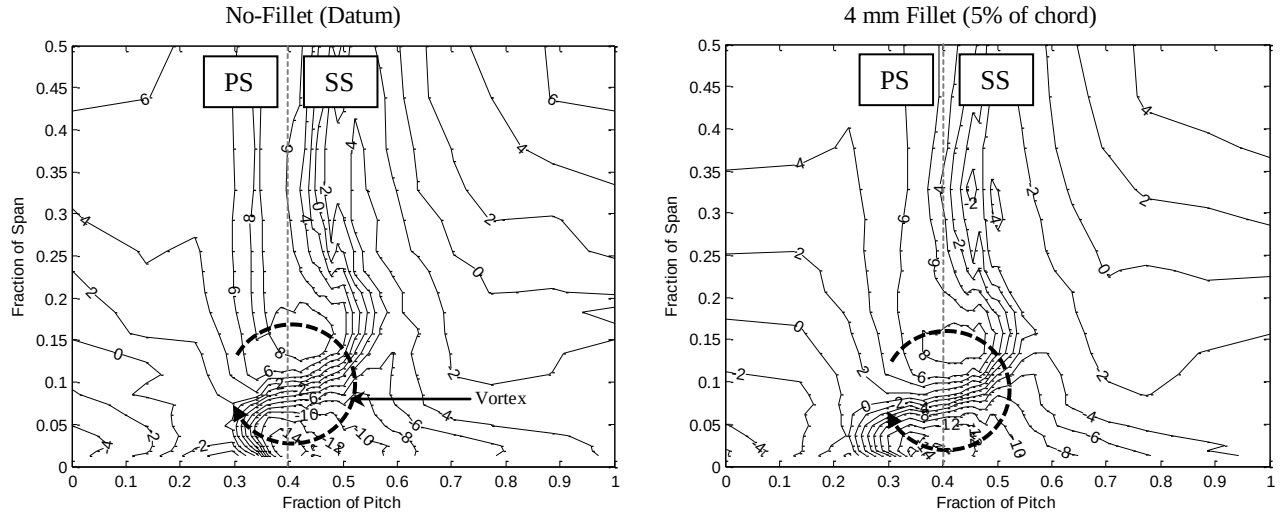

Fig. 4 (contd.): Contours of flow angle for different tip gaps at cascade exit (70% blade chord from trailing edge)

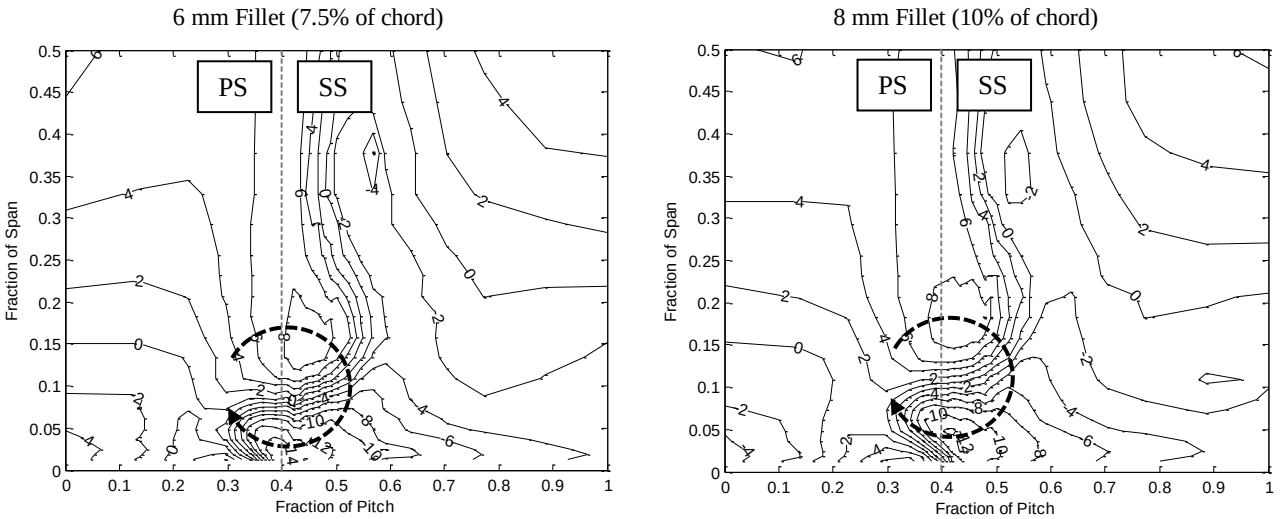

Fig. 4: Contours of flow angle for different tip gaps at cascade exit (70% blade chord from trailing edge)

The wake width across the loss-core itself remains approximately the same for all cases. Since the area traverse data is collected using a 3-hole probe, only the axial and pitchwise information is available, thus, making it difficult to quantify vortex related information. However, the contours of circumferential flow angle (α) as presented in Fig. 4 are able to give us some information on the secondary vortex. Consistent with the classical observations a vortex with an anti-clockwise sense is seen for all the four test cases as indicated by the black arrows. Notably, the spanwise location of these vortices (near the 10% span region) is much lower than where the loss-cores were found (from 24 to 28% of span) in Fig. 3. The variation in the spanwise location of the approximate vortex centre for the different fillet sizes, as indicated by the flow angle contours, follows the same trend as that for the loss-core. The vortex moves closer to the endwall with the 4 mm fillet than for the no-fillet case and progressively moves away from the wall as the fillet radius is increased to 6 mm and 8 mm.

How close the flow angle contour lines are packed in the vicinity of the vortex is a good indication of the vortex strength in that an increased contour line density (i.e. closely packed contours) indicates a stronger vortex. This would then suggest that as the fillet size is increased the vortex becomes weaker. This observation is in line with the findings within turbines as mentioned earlier in the paper and that by Kügeler et al [6] in a multistage compressor. The spanwise distributions of mass averaged total pressure loss and circumferential flow angle are presented in Fig. 5. At first, the loss coefficient distribution for the various fillet radii cases look very alike and a closer observation is required to differentiate between them. Two distinct regions could be identified; the near-wall region in the first 10% of span as indicated by the shaded portion and the region that is outside of this. In the near-wall region the lowest total pressure loss coefficient values are found to be associated with the highest fillet radii. The loss values marginally increase as the fillet radius is reduced.

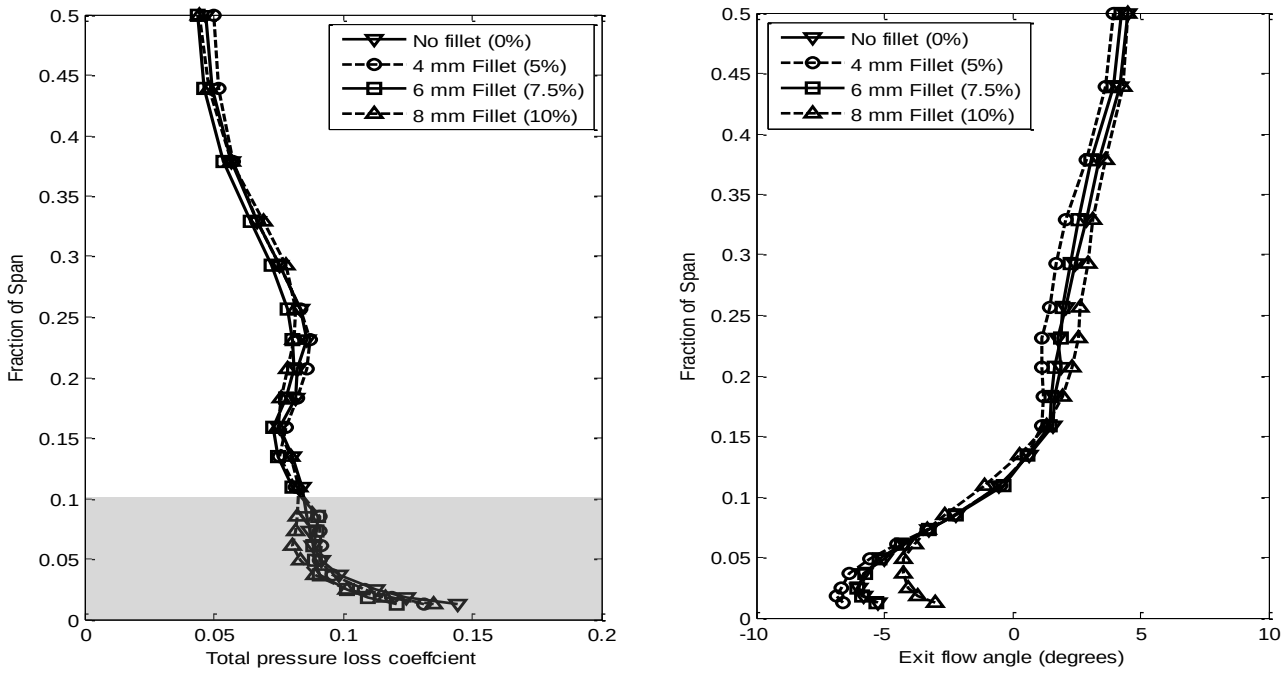

Fig. 5: Spanwise distribution of pitchwise area averaged total pressure loss coefficient and flow angle at cascade exit (the shaded region represent the inner 10% of span over which the near-wall loss is estimated)

In the outer region, however, the picture is not that straight forward, but the cases with a fillet have generally lower losses than the one without a fillet. The lowest loss in this region is observed for the 6mm fillet (7.5% of chord), which, significantly, has the same height as the inlet boundary layer. In the spanwise flow angle distribution plot a similar difference between the near-wall and outer region is visible. Notably, in the inner 10% of span the overturning due to the secondary flow is greatly reduced for the larger fillets. This is a good indication of the reduction in the cross flow when fillet is added which was observed by previous researchers. This however contradicts with what was reported by Meyer et al [8] who tested blades with identical shapes but at a much higher Reynolds number. The above authors reported an increased cross flow which they then attributed to a reduction in axial velocity and the consequent increase in static pressure rise that they observed. A clearer picture emerges when mass/area averaged quantities over the whole of the traverse area is presented and plotted against the corresponding fillet sizes.

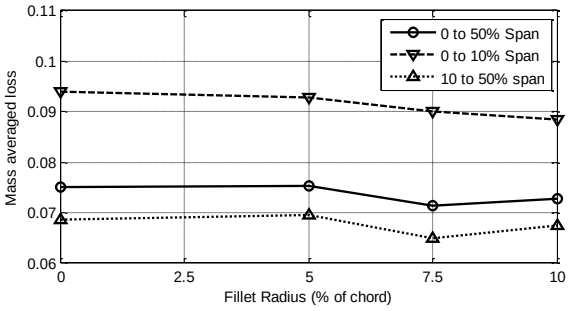

Fig. 6: Mass averaged loss calculated over 50% span

Fig. 6 shows the mass averaged values of the total pressure loss coefficient for the no-fillet case and the three fillet radii cases tested. Note that the mass average is not performed over the entire span as the area traverse was only carried out between the endwall and the mid-span location (i.e. 0 to 50% span). The averaged loss over the 0-50% span region is seen not to change much by the addition of the smallest of the fillets tested with 4mm radius. However, with a 6mm fillet, the loss coefficient value reduced by 5% of its value for the no-fillet case. With the 8mm fillet, the loss coefficient value has slightly increased but still 3% less than its value for the no-fillet case. The loss coefficient value evaluated (mass weighted) over the inner 10% (shaded region in Fig. 5) and the outer region (10-50%) are also shown in Fig. 6. What is immediately clear, not surprisingly, is that the mass weighted loss in the near-wall region is much higher (approximately 35%) than those in the outer region. The values for the outer region trends exactly similar to the average loss in the entire traverse area as discussed above with the lowest loss co-efficient value associated with the 6mm fillet.

In the inner region, however, the loss coefficient reduces by 1.5%, 4% and 6% respectively for the 4mm, 6mm, and 8mm radius cases on its value compared to the no-fillet case. This is thought to be a result of the reduced cross flow as indicated by the reduced overturning as the fillet size is increased and the resulting reduction in the extent of the hub separation. This observation is well backed up by the findings of Goodhand and Miller [7] who demonstrated the reduction in the spanwise extent of the separated region using flow visualisation on the stator of a 1.5 stage low speed compressor that was tested with fillet radii of different sizes. Another averaged quantity that is worth looking at is the static pressure rise coefficient (ψ) as plotted in Fig. 7.

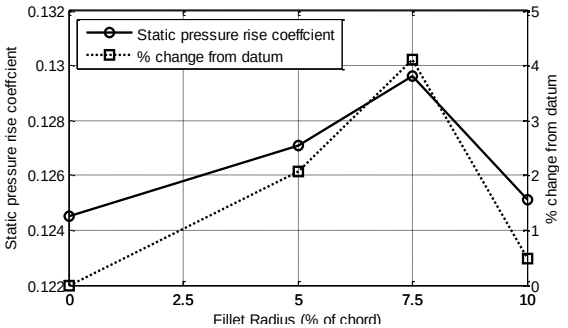

Fig. 7: Static pressure rise coefficient calculated over 50% span

Meyer et al [8] noted in their study, at a higher Reynolds number, that the static pressure rise increased with fillet radius for all radii below the height of the inlet boundary layer (δ), which as mentioned earlier in the paper was attributed to a reduced axial velocity due to increased cross flow. In the present measurements, however, all filleted cases showed a higher static pressure rise coefficient value with the highest gain materialising at a fillet height of 6mm which is also the height of the inlet boundary layer. The pressure rise is seen to increase from its value for the no-fillet case by 2% for the 4mm and then by 4% for the 6mm fillet case beyond which it reduces for the 8mm case, but, interestingly, still higher than that for the no-fillet case by 0.5%. As with the spanwise variation of the total pressure loss coefficient, it is argued that the increased static pressure rise is not a local effect but an effect of the reduced secondary flow at larger fillet radii on flow over the entire blade span. The uncertainty in the measurement of flow angle is better than 0.5° and that in determining the values of the pressure coefficients only better than 0.005. Although the trends presented here are likely to be true and hence back up the physical explanations that are provided, the exact values presented should be taken in this context.

4. Conclusions

The literature survey for this paper suggested that there is no comprehensive physical understanding yet of the effect of blade fillets on the aerodynamics of the compressor. While some of the studies showed very minimal effects due to the presence of fillets others noted an increased loss with larger fillet radii. Some found a better blade-row performance at increased incidence (off-design) when fillets are present but reduction in loss at design point was also reported with fillets. It is apparent that blade loading may be an important factor in determining how sensitive the aerodynamics is to the use of fillets. It is also possible that some of the contrasting results reported could be

explained using the level of loading applied. The scope of the present study was however limited and the primary objective here was to look at the effect of fillets at a relatively low Reynolds number. The following conclusions could be drawn from this study:

- The presence of the fillet weakens cross passage flow and reduces overturning of the endwall flow.
- When fillets are present, indication is that the vortex is much weaker.
- A clear reduction in losses near the endwall is seen as the fillet size increases.
- Overall, losses were measured to be lower for all fillet sizes tested compared to the no-fillet case.
- The increase in loss with fillet size is not monotonic since the lowest loss was found when the fillet height is the same as that of the incoming boundary-layer.
- The measured static pressure rise coefficient is higher for all filleted cases compared to the no-fillet case achieving a maximum for the fillet with the same size as the inlet boundary layer.
- The static pressure rise increase is not thought to be local to the endwall region but is a result of reduced secondary flow and corner separation and its effect on the entire blade span.
- The trends of the loss reduction and the static pressure rise observed with the addition of fillets in the present study suggests that both of the above advantages could disappear when larger fillets are employed than those tested here. A fillet of the same height as the incoming boundary layer is found to be the most effective.
- Inlet boundary layer height is observed to have an effect on the loss and pressure rise but further investigation is needed to understand the physical reasons behind this observation.

ACKNOWLEDGEMENTS:

The work described in this paper is a result of multiple student projects supervised by the author at the University of Sussex. The author would wish to thank the Department of Engineering and Design at Sussex for funding the experiment hardware through projects. More importantly thanks are due to the project students; Jonathan, Glen, Omar and Laurence who took part in the hardware design/set-up and the testing at various stages. The author would also like to thank Meyer et al [8] for providing with the coordinates of the aerofoil.

REFERENCES:

[1] G.A. Zess and K.A. Thole. 2002. Computational design and experimental evaluation of using a leading edge fillet on a gas turbine, *ASME J. Turbomachinery*, 124(2), 167-175. http://dx.doi.org/10.1115/1.1460914.

[2] T. Germain, M. Nagel, I. Raab, P. Schuepbach, R.S. Abhari, M.G. Rose. 2008. Improving efficiency of a high work turbine using non-axisymmetric endwalls part I: Endwall design and performance, *ASME Paper*, GT2008-50469.

[3] O. Turgut and C. Camci. 2012. Experimental investigation and computational evaluation of contoured endwall and leading edge fillet configurations in a turbine NGV, *ASME Paper*, GT2012-69304.

[4] S. Mank, M. Hilfer, R.J. Williams, S.I. Hogg and G.L. Ingram. 2014. Secondary flows and fillet radii in a linear turbine cascade, *ASME Paper*, GT2014-25458.

[5] B.P. Curlett. 1991. *The Aerodynamic Effect of Fillet Radius in a Low Speed Compressor Cascade*, NASA-TM-I05347.

[6] E. Kügeler, D. Nürnberger, A. Weber and K. Engel. 2008. Influence of blade fillets on the performance of a 15 stage gas turbine compressor, *ASME Paper*, GT2008-50748.

[7] M.N. Goodhand and R.J. Miller. 2012. The impact of real geometries on three-dimensional separations in compressors, *ASME J. Turbomachinery*, 134, 021007, 1-8. http://dx.doi.org/10.1115/1.4002990.

[8] R. Meyer, S. Schulz, K. Liesner, H. Passrucker and R. Wunderer. 2012. A parameter study on the influence of fillets on the compressor cascade performance, *J. Theoretical and Applied Mechanics*, 50(1), 131-145.